Comm. in Asteroseismology
Vol. 153, 2008

CCD photometry of δ Scuti stars 7 Aql and 8 Aql

L. Fox Machado[1], R. Michel[1], M. Álvarez[1], L. Parrao[2],
A. Castro[1], and J. H. Peña[2]

[1] Observatorio Astronómico Nacional, Instituto de Astronomía,
Universidad Nacional Autónoma de México,
Ensenada B.C., Apdo. Postal 877, México
[2] Instituto de Astronomía, Universidad Nacional Autónoma de México,
México D.F., Apdo. Postal 70-264, México

Abstract

As a continuation of the study of the δ Scuti stars 7 Aql and 8 Aql, new CCD photometric data were acquired in 2007. We present a period analysis of these data that confirms the dominant modes detected in each star in the framework of the STEPHI XII campaign in 2003.

Individual Objects: 7 Aql, 8 Aql, GSC 05118-00503, GSC 05118-00553,
GSC 05118-00513

Introduction

δ Scuti variables are promising candidates for helping our understanding the internal processes occurring in the interiors of intermediate mass stars. Most of the δ Scuti stars pulsate, simultaneously, in a number of radial and non-radial modes showing complicated pulsation spectra. Since long time series are required to disentangle their pulsation spectra, multisite coordinated campaigns are often undertaken (e.g., STEPHI, Stellar Photometry International, Michel et al. 2000 or Delta Scuti Network, Breger et al. 1999), and space observations are underway (COROT, Baglin 2003, Michel et al. 2005).

7 Aql (HD 174532, SAO 142696, HIP 92501) is a δ Scuti variable discovered in a systematic search and characterization of new variables in preparation for the COROT mission (Poretti et al. 2003), and was selected as the main target of the STEPHI XII multisite campaign in 2003. In this campaign, 8 Aql (HD 174589, SAO 142706, HIP 92524) was used as the only comparison star because no other bright stars are in the field-of-view (FOV) of the 4-channel photometer used in the STEPHI network.

Nonetheless, by carefully analyzing the derived differential light curve of 7 Aql and 8 Aql and individual nondifferential light curves, we were able to demonstrate that

Table 1: Positions, magnitudes and spectral type of targets and comparison stars.

Star	ID	RA (2000.0)	Dec (2000.0)	V (mag)	SpTyp
7 Aql	HD 174532	18 51 05	-03 15 40.1	6.9	A2
8 Aql	HD 174589	18 51 22	-03 19 04.2	6.1	F2
C1	GSC 05118-00503	18 51 09	-03 18 52.2	12.6	-
C2	GSC 05118-00553	18 51 04	-03 18 36.1	13.6	-
C3	GSC 05118-00513	18 51 02	-03 17 32.5	12.1	-

8 Aql is a new δ Scuti variable. Moreover, it was shown that the amplitude spectrum of both stars are not superposed. Three and seven frequency peaks were unambiguously detected with a 99% confidence level in 8 Aql and 7 Aql respectively and a possible identification of the observed modes in terms of radial order was performed (Fox Machado et al. 2007).

As a continuation of this study, we have carried out CCD photometric observations in 2007 of 7 Aql and 8 Aql to obtain differential photometry of these stars with respect to a much dimmer comparison star. The primary results of these observations are present in this paper.

Observations and data reduction

CCD photometric observations of 7 Aql and 8 Aql were carried out for fourteen nights (about 86 hours of data) over the periods of June 14 to 21 and July 7 to 12, 2007, at the Observatorio Astrónomico Nacional, in San Pedro Mártir, Baja California, México. The observations were performed using the 0.84 m telescope to which a CCD camera was attached. A 1024×1024 CCD camera was used in June with a plate scale of $0.38''$/pixel, while a 2048×2048 camera was implemented in July which has a plate scale of $0.15''$/pixel. The observations were obtained through a Johnson V filter.

Figure 1 shows a typical image of the CCD's FOV ($7.5' \times 7.5'$ at the f/15 focus of the telescope) during the observing runs. This FOV supplies a large set of reference stars for the two variables. We have selected, however, the brighter ones after 7 Aql and 8 Aql for computing differential magnitudes. The coordinates, V magnitudes and identifications of the reference stars (marked as C1, C2, and C3 in Figure 1), and main targets are listed in Table 1. Pieces of gelatin neutral density filter (Kodak Wratten ND 2.0) with a transmission of $\sim 1\%$ placed on top of the V filter (the dark regions in Figure 1) were used to reduce the brightness of the variable stars at the detector since, as can be seen in Table 1, they are much brighter than the selected comparison stars in the CCD's FOV. This allowed us to obtain images with high signal-to-noise (S/N) ratios in both the pulsating and comparison stars with an exposure time of about 90 s without reaching the saturation levels of the CCD detectors. The acquired images were reduced in the standard way using the IRAF package. Aperture

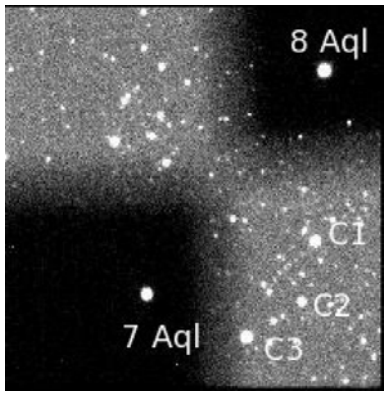

Figure 1: Image of the CCD field-of-view ($7.5' \times 7.5'$). The reference stars are marked as C1, C2 and C3. North is down and East is right.

photometry was implemented to extract the instrumental magnitudes of the stars. All differential magnitudes have been computed using GSC $05118-00503$ (C1) as the principal comparison star and GSC 05118-00553 (C2) as the check star. GSC 05118-00513 (C3) was useful neither as comparison nor as check star because, as can be seen in Figure 1, in some CCD images it was so close to the neutral density filter that its magnitude was affected. The differential magnitudes were normalized by subtracting the mean of differential magnitudes for each night.

The differential light curves 8 Aql - C1, 7 Aql - C1 for three selected nights are illustrated in Figure 2 (the three top and three middle plots respectively). As can be seen, the oscillations of 8 Aql and 7 Aql are clearly inferred, with the dominant period of 8 Aql longer than that of 7 Aql. The magnitude differences between comparison stars C1 - C2 were also derived to confirm their constancy. As can be seen in Figure 2 (the three bottom plots), no indications of photometric variability on these stars was found.

Frequency analysis

The amplitude spectra of the differential time series were obtained by means of an iterative sinus wave fit (ISWF; Ponman 1981) and the software package Period04 (Lenz & Breger 2005). In both cases, the frequency peaks are obtained by applying a non-linear fit to the data. Since both packages yielded similar results, we present the spectral analysis only in terms of ISWF. The window function of the observations is shown in Figure 3. As is known, observations from a single site yield a worse window function as compared to multisite observations, hence the sidelobes in the spectral window are at 90% of the main lobe. Even so, the resulting amplitude spectra are good enough to determine the main pulsation modes in each star.

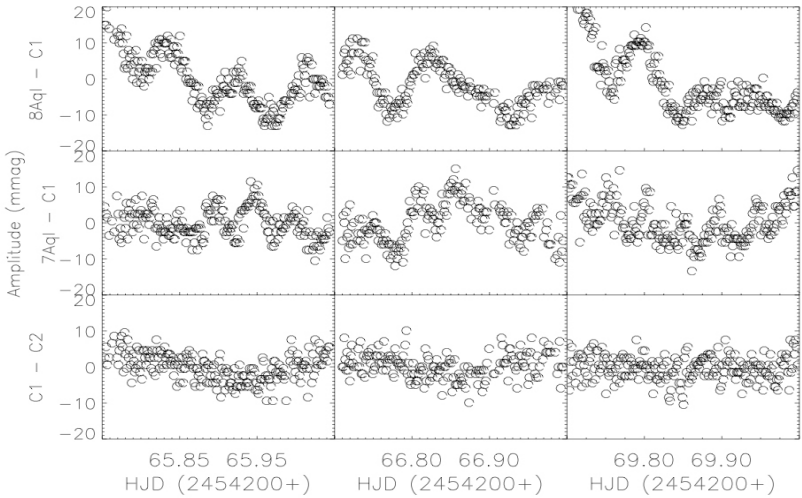

Figure 2: Examples of the differential light curves with reference star 'C1'. The three top and middle plots correspond to differential light curve 8 Aql - C1 and 7 Aql - C1 respectively. The three bottom plots are for C1 - C2.

The amplitude spectra of the differential light curves 8 Aql-C1 and 7Aql-C1 are shown in the top panel of Figure 4 and Figure 5, respectively. We note that below 100 μHz these spectra are dominated by the daily aliasing. A quick inspection of these spectra in the region $> 100\,\mu$Hz shows that the amplitude spectrum of 8 Aql present the main peaks between 100 and 200 μHz, while in the amplitude spectrum of 7 Aql the peaks are between 200 and 300 μHz. The subsequent panels in the figures, from top to bottom, illustrate the prewhitening process of the frequency peaks in each amplitude spectrum. We followed the same procedure as explained in Álvarez et al. (1998). In the case of 8 Aql (Figure 4), the highest amplitude peak is located at 143.36 μHz, but after prewhitening the peak at 11.69 μHz. This latter is most likely to be the first harmonic of the day and it is not considered hereafter. On the other hand, 7 Aql (Figure 5) shows a frequency peak at 235.96 μHz. Both frequency peaks are confirmed in the amplitude spectrum of 8 Aql - 7 Aql (Figure 6) after prewhitening the peak at 11.69 μHz. The remaining peaks, which seem to be weakly present in all amplitude spectra, may be disregarded because they do not significantly improve the residuals. These peaks are indistinguishable due to the aliasing caused by the window function. In any case, our goal was to detect the main pulsation modes in each star. Figure 7 illustrates the amplitude spectra C1 - C2. As can be seen, the typical $1/f$ noise dominates whole spectrum. It confirms the non-oscillatory behavior in both stars.

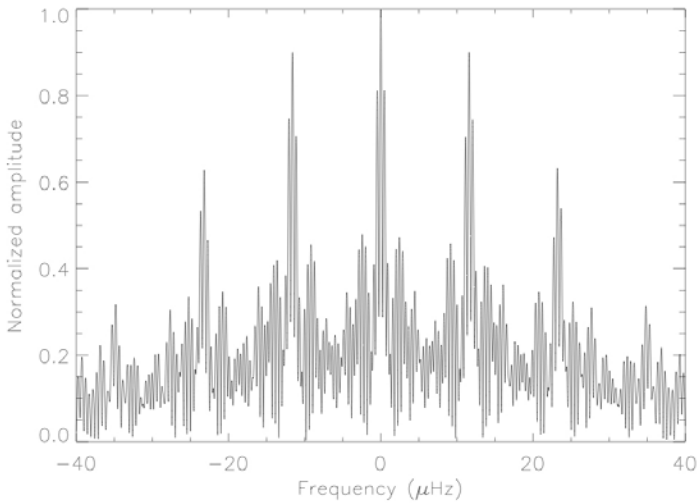

Figure 3: Spectral window in amplitude. The first sidelobes are at 90% of the main lobe.

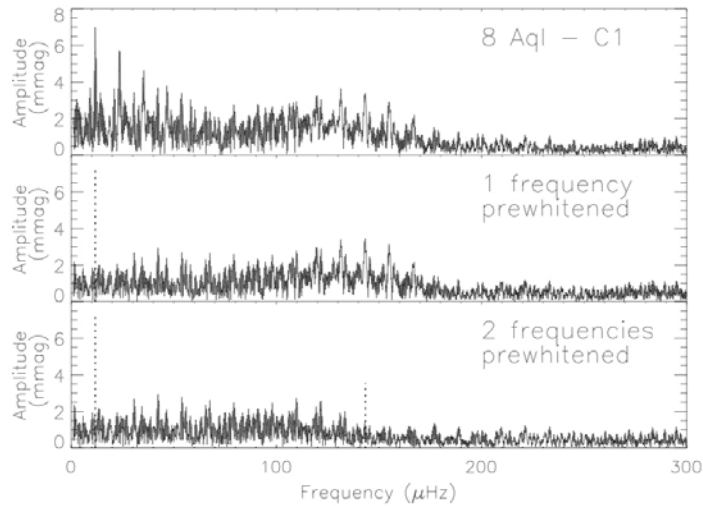

Figure 4: Amplitude spectrum 8 Aql - C1 and the prewhitening process of the detected peaks.

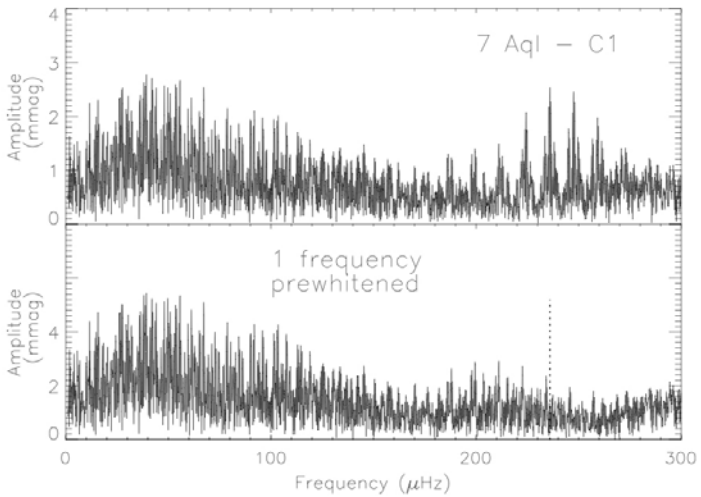

Figure 5: Amplitude spectrum 7 Aql - C1 and the prewhitening process of the detected peaks.

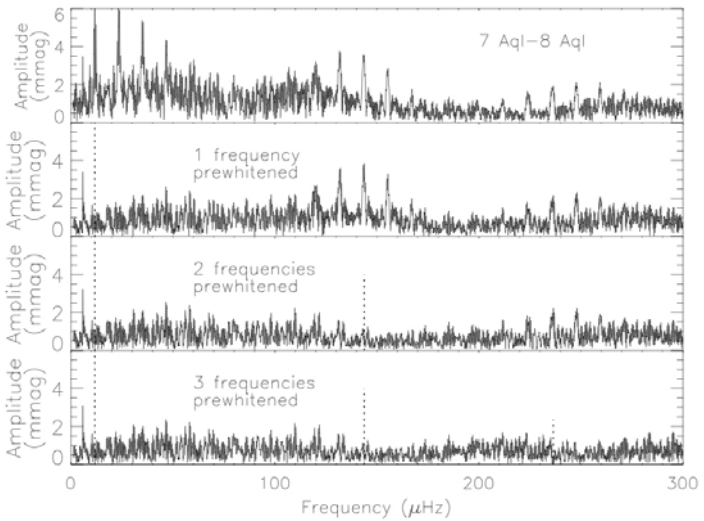

Figure 6: Amplitude spectrum 7 Aql - 8 Aql and the prewhitening process of the detected peaks.

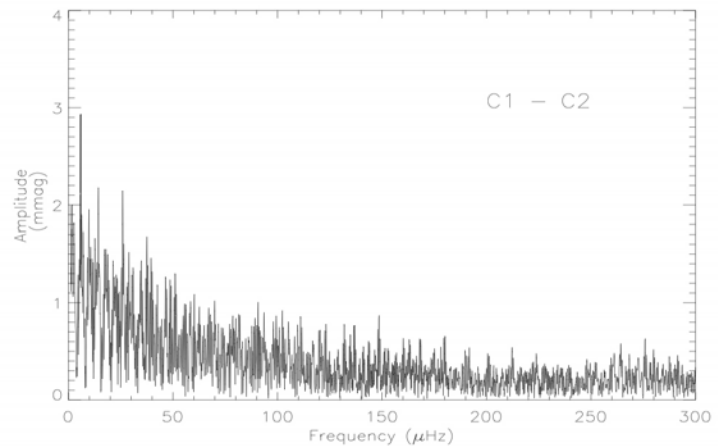

Figure 7: Amplitude spectrum C1 - C2.

Table 2: Detected frequencies in the present study and the dominant modes detected in the STEPHI XII campaign. $\nu_{\rm a}$ is the first harmonic of the day.

This paper (2007)				STEPHI XII (2003)			
	ν (μHz)	A (mmag)	S/N		ν (μHz)	A (mmag)	S/N
	8 Aql - C1				*8 Aql*		
$\nu_{\rm a}$	11.69	7.4	-	$\nu_{\rm a}$	-	-	-
ν_1	143.36	3.6	3.0	ν_1	143.36	9.8	7.9
	7 Aql - C1				*7 Aql*		
ν_1	235.96	2.6	3.8	ν_1	236.44	5.8	5.5
	7 Aql - 8 Aql				*7 Aql - 8 Aql*		
$\nu_{\rm a}$	11.69	9.2	-	ν_a	-	-	-
ν_2	143.76	4.0	3.7	ν_2	143.36	9.8	15.7
ν_3	236.45	2.4	3.0	ν_3	236.44	9.6	9.9

Discussion

The frequencies, amplitudes and S/N ratio in amplitude of the peaks detected in the amplitude spectra 7 Aql − C1 (Figure 4), 8 Aql − C1 (Figure 5) and 7 Aql − 8 Aql (Figure 6) are summarized in Table 2. For comparison, the dominant modes detected in nondifferential and differential time series derived in the STEPHI XII campaign are also shown. It is evident that the dominant modes detected in each star in the STEPHI XII campaign are confirmed. There is a fairly good agreement between the frequency values derived in this survey and those derived from multisite photoelectric photometry, besides that the sigle-site observations are less accurate than the multisite observations. The disagreement in the amplitudes can be attributed to the much slower sampling rate of the CCD detectors. In fact, this might have suppressed not only the amplitude of the main oscillation modes but also the secondary harmonics found in the STEPHI XII campaign.

Conclusions

We have presented the analysis of new CCD photometric observations of δ Scuti stars 7 Aql and 8 Aql carried out during fourteen nights in June and July, 2007 at the Observatorio Astronómico Nacional, México. About 86 hours of time resolved CCD differential photometry were obtained. The dominant oscillation frequencies detected in 2003 in the framework of the STEPHI XII campaign by means of nondifferential photometry have been confirmed in this season by using CCD differential photometry.

Acknowledgments. We would like to thank the staff of the OAN for their assistance during the observations. This paper was partially supported by Papiit IN108106.

References

Alvarez, M., Hernandez, M. M., Michel, E., et al. 1998, A&A 340, 149

Baglin, A. 2003, AdSpR. 32, 345

Breger, M., Handler, G., Garrido, R., et al. 1999, A&A 349, 225

Fox Machado, L., Michel, E., Prez Hernndez, F., et al. 2007, AJ 134, 860

Lenz, P., & Breger, M. 2005, CoAst 146, 53

Michel, E., Chevreton, M., Belmonte, J. A., et al. 2000, ASPC 203, 483

Michel, E., Auvergne, M., Baglin, A., et al. 2005, ASPC 333, 265

Ponman, T. 1981, MNRAS 196, 583

Poretti, E., Garrido, R., Amado, P. J., et al. 2003, A&A 406, 203